18TH WORLD CONFERENCE ON EARTHQUAKE ENGINEERING
WCEE2024
MILAN

MILAN, ITALY
30TH JUNE - 5TH JULY 2024

www.wcee2024.it

ESTIMATING FIRST AND HIGHER-MODE EFFECTS FOR THE DESIGN OF ROCKING MASS TIMBER WALLS WITH CONTROLLED OVERTURNING MOMENTS

L. Pieroni[1*,2], G.A. Araújo R.[2], B. Simpson[2], F. Freddi[1], P. Mishra[3], P. Uarac[4], A. R. Barbosa[4], A. Sinha[4], J.W. van de Lindt[3], N. Brown[5]

[1] University College London, London, UK, *ludovica.pieroni.20@ucl.ac.uk

[2] Stanford University, Stanford, US

[3] Colorado State University, Fort Collins, US

[4] Oregon State University, Corvallis, US

[5] The Pennsylvania State University, University Park, US

Abstract

To address functional recovery after earthquakes, there is growing interest in developing enhanced-performance seismic-resisting systems. Rocking walls, featuring a base gap-opening mechanism and designed to remain essentially elastic above the base, have demonstrated their potential in various construction materials, including mass timber. If combined with steel energy dissipators, the resulting hybrid steel-mass timber rocking walls have emerged as a promising seismic-resisting system. This study focuses on Post-Tensioned Mass Timber Rocking Walls supplemented with Buckling-Restrained Brace (BRB) boundary elements and builds upon findings from experimental programs funded by the National Science Foundation (NSF) and the United States Department of Agriculture (USDA). The rocking mechanism, controlled by the BRBs and the Post-Tensioned (PT) rods, provides self-centering behaviour, reducing the potential for residual drifts and improving post-earthquake repairability. An estimating method for higher-mode loading profiles is proposed and applied to a six-story archetype, which was tested at the Large High Performance Outdoor Shake Table (LHPOST) at the University of California San Diego (UCSD) in January 2024 as part of the NHERI Converging Design Project. The estimating method is practically formulated to facilitate the implementation in design procedures.

1 Introduction

Past seismic events have resulted in large direct and indirect financial losses associated with repair costs and extensive downtime (EERI 2019). As a result, there has been increased interest among engineers and government agencies to develop enhanced-performing seismic-resisting systems that achieve functional recovery, reducing the probability of post-earthquake damage and downtime (Terzic *et al.* 2021, Cook *et al.* 2022, Molina Hutt *et al.* 2022). As mass timber seismic-resisting systems are only now starting to be codified (FEMA P-2082-1 2020, IBC 2020, SDPWS AWC 2021, ASCE 7 2022), there is a unique opportunity to pioneer a high-performance design paradigm aimed at minimizing casualties and economic losses after strong ground shaking.

Hybrid steel-mass timber rocking walls have emerged as a promising design solution that combines the aesthetic and environmental benefits of timber with the ductility and stable energy dissipation properties of steel components. Rocking walls have been proposed for various construction materials, such as reinforced

concrete (Restrepo & Rahman 2007, Panagiotou *et al.* 2011), masonry (Yassin *et al.* 2022), steel (Tremblay *et al.* 2014, Takeuchi *et al.* 2015, Simpson & Mahin 2018), and mass timber (Loo *et al.* 2014, Sarti *et al.* 2016, Akbas *et al.* 2017, Pei *et al.* 2019, Chen *et al.* 2020, Granello *et al.* 2020, Araújo *et al.* 2022, Wichman *et al.* 2022 a,b). These walls consist of a stiff and strong vertical element that runs continuously along the height of the building. They are designed to remain essentially elastic above the base, leading to a more even distribution of drifts along the building's height. The rocking behaviour at the base is accomplished by intentionally reducing the flexural capacity at the base and allowing a gap-opening mechanism. Energy dissipators can be used to control the overturning moment, *e.g.,* Buckling-Restrained Brace (BRB) boundary elements (Takeuchi *et al.* 2015, Bosco *et al.* 2018, Araújo *et al.* 2022, Jiang *et al.* 2022). Post-Tensioning (PT) of the wall through high-strength steel rods can be used to control the self-centering mechanism, thereby reducing residual drifts and meeting the functional recovery objectives (Sarti *et al.* 2016, Loo *et al.* 2014, Pei *et al.* 2019, Chen *et al.* 2020, Wichman *et al.* 2022 a, b).

Current seismic standards in the U.S. and Europe primarily focus on mass timber non-continuous vertical walls with standardized connections (ASCE 7 2022, SDPWS AWC 2021, FEMA P-2082-1 2020, IBC 2020) excluding many proposed design alternatives and necessitating performance-based design approaches. Importantly, general design methodologies for rocking walls must account for the unique higher-mode behaviour observed in these systems (Wiebe & Christopoulos 2009, Panagiotou & Restrepo 2009, Roke *et al.* 2009, Chen *et al.* 2017, Chen *et al.* 2018, Martin & Deierlein 2019, Sanscartier *et al.* 2019, Simpson 2020, Simpson & Rivera Torres 2021, Christopoulos & Zhong 2022). The design forces for the rocking walls arise from two sources. In the first mode, the forces are limited by the strength of the energy dissipators that control the overturning moment. In the higher modes, the forces increase near-linearly with story drifts, because shears and moments in the wall are designed to remain elastic in all modes. This response is typical of rocking walls and is referred to as *near-elastic higher-mode effects.* The distinct dynamic behaviour needs to be considered when estimating the seismic demands of rocking walls.

Displacement-based and force-based design methods have been proposed for rocking mass timber walls (Pang *et al.* 2010, Loss *et al.* 2018; Huang *et al.* 2021, Uarac *et al.* 2022, Busch *et al.* 2022). Unlike performance-based design approaches that require nonlinear analysis, these procedures use techniques that can be routinely applied in design practice providing a basis for the prescriptive design of mass timber rocking walls. Nevertheless, they do not explicitly incorporate design criteria for the unique dynamic characteristics of these systems (*i.e.,* higher mode effects), which are left to the rational analysis of the structural engineer. In the literature, various methods for estimating near-elastic higher-mode effects were proposed (Eberhard & Sozen 1993, Eibl & Keintzel 1988, Roke *et al.* 2009, Panagiotou & Restrepo 2011, Wiebe & Christopoulos 2015, Steele & Wiebe 2016). Alternative design procedures, including strategies to estimate near-elastic higher-mode effects, would add to the available design practices that engineers can use for the seismic design of rocking walls.

In this study, an estimating method for modal periods and mode shapes is proposed for PT Mass Timber Rocking Walls with controlled overturning moments using BRBs as energy dissipators. The estimates were applied to a six-story archetype located in Seattle, WA, which was tested at full-scale in the Large High Performance Outdoor Shake Table (LHPOST) at the University of California San Diego (UCSD) in January 2024 as part of the NHERI Converging Design Project. To compare results to eigenvalue analyses, a 2D numerical model of the archetype was developed in OpenSeesPy. It is expected that the estimating method can be eventually extended to generically design rocking archetypes in various construction materials.

2 Rocking walls with controlled overturning moments

Figure 1 (a) shows the seismic-resisting system investigated in the present paper. It consists of Post-Tensioned Mass Timber Rocking Walls supplemented with BRB boundary elements. In these systems, the BRBs dissipate the seismic energy, and the rocking mechanism limits residual drifts. The gap-opening mechanism at the base of the wall engages the PT rods in tension and the BRBs in both tension and compression, providing forces that balance the overturning moment at the base. The design of the seismic-resisting systems is based on the following criteria at the Design Earthquake (DE) and Risk-Targeted Maximum Credible Earthquake (MCE_R) levels:

- Self-centering behaviour is achieved by designing the overturning moment due to the PT rods and the gravity load to be higher than the overturning moment due to the BRBs. The PT rods are expected to remain elastic at the DE level;
- The inelastic response of the system is limited to the yielding of the BRBs, plus a minor inelastic response in the wall at the rocking interface at the DE level;
- The mass timber wall remains essentially elastic above the base in all modes of vibration even at the MCE_R level targeting a near-uniform distribution of drifts across all stories.

To meet the design criteria, the design procedure of PT Mass Timber Rocking Walls includes the following steps: i) sizing of the energy dissipators and PT rods, ii) estimate of the mode shapes and modal periods of the system, iii) stiffness check on the wall based on the first-mode period, and iv) strength check on the wall based on seismic demands estimates.

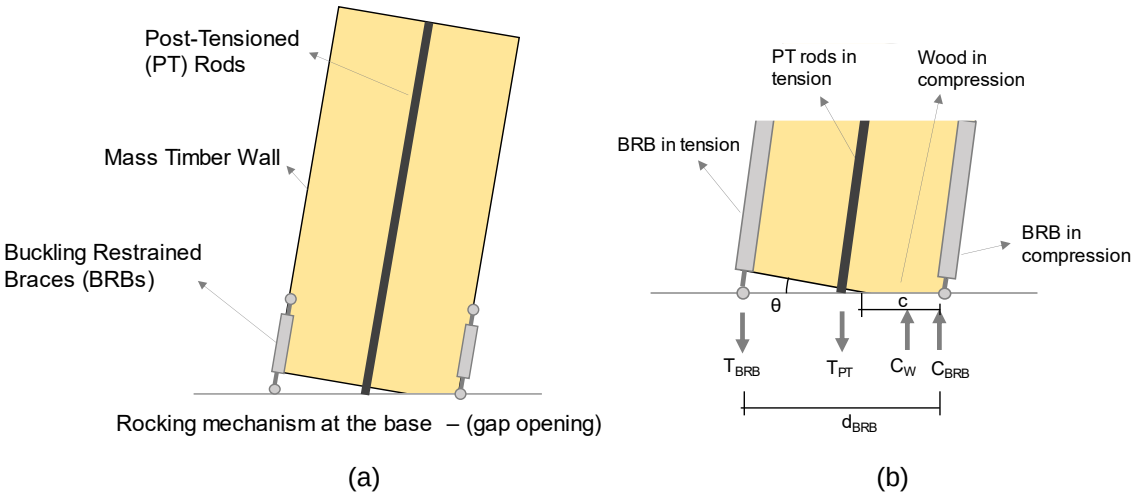

Figure 1. Schematic of: (a) Post Tensioned Mass Timber Rocking Walls with BRBs. (b). Forces in the rocking interface at yielding of the BRB in tension.

3 Design and mode estimates

The energy dissipators and PT rods (*i.e.,* deformation-controlled elements) can be designed by traditional means to meet the demand of the DE level using the Equivalent Lateral Force (ELF) procedure described in ASCE 7 (2016) and (2022). Additionally, to achieve the full self-centering behaviour, the overturning moment due the PT rods (M_{PT}) and the gravity load on the wall (M_G) needs to exceed the overturning moment due to the BRBs (M_{BRB}), including the expected overstrength due to kinematic and isotropic hardening of the BRBs (Palermo 2007, Pampanin *et al.* 2001, Busch *et al.* 2022, Pieroni *et al.* 2022). The definition of the quantities M_{PT}, M_G and M_{BRB} are described in the following section. After sizing of the BRBs and PT rods, the wall is proportioned to meet specific stiffness and strength criteria to remain predominantly elastic in all vibrational modes, relying on the yielding of the BRBs for energy dissipation and the elastic behaviour of PT rods for self-centering. To perform stiffness and strength checks on the wall, the mode shapes and the modal periods need to be estimated.

Section 3.1 describes the proposed estimating method for mode shapes and modal periods, while 3.2 presents the stiffness and strength checks.

3.1 Estimates of the mode shapes and modal periods

When subjected to seismic loading, rocking walls lose rotational stiffness at the base due to rocking. After the activation of the gap-opening mechanism, there are various factors affecting the stiffness at the base, such as the drift demand, the force in the BRBs, the force and stiffness in the PT rods, and the position of the center of rotation which may change during the motion. Medium- to high-rise rocking systems with this kind of behaviour can be generalized and preliminary estimated using a cantilever beam analogy (Wiebe *et al.* 2015, Chen *et al.* 2017, Chen *et al.* 2018). This approach idealizes the wall as a cantilever beam with uniform mass and stiffness along the height, and with a rotational spring of finite stiffness as base restrain. Additionally, the

approach assumes that the structural response is dominated by flexural-type deformations or by shear-type deformations.

The proposed estimating method separates the behaviour of the rocking wall into two contributions (Figure 2): (i) a pure-shear cantilever beam fixed at the base, (ii) a pure-flexural cantilever beam with rotational spring at the base of limited stiffness.

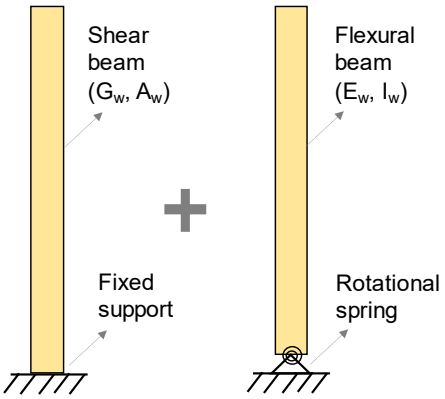

Figure 2. Shear and flexural contributions to estimate mode shapes and modal periods for rocking walls.

Estimates of the mode shapes ($\phi_n(z)$) are defined using the solution of the equation of motion for flexural beams with a rotational spring at the base of limited stiffness (k_r) as follows:

$$\phi_n(z) = C_n(\cosh(\beta_n z) - \cos(\beta_n z) + A_{nsin}\sin(\beta_n z) - A_{nsinh}\sinh(\beta_n z)) \quad (1)$$

where $\phi_n(z)$ is the n^{th} mode shape, z is the vertical coordinate along the height of the wall, β_n, $A_{n,sin}$, and $A_{n,sinh}$ are modal constants associated with the stiffness of the rotational spring at the base (k_r) and calculated for each mode (Wiebe *et al.* 2015). The modal period of the n^{th} mode ($T_{n,f}$) for the flexural beam with a rotational spring of limited stiffness at the base can be calculated based on the modal constant β_n.

In the proposed estimating method, the base partial restraint is determined at the yielding of the BRB in tension, assuming the wood in the wall's toe is elastic in compression. Hence, the stiffness of the rotational spring at the base (k_r) is calculated as follows.

$$k_r = \frac{M_b}{\theta} = \frac{M_{BRB,tens} + M_{PT} + M_{BRB,comp} + M_{wood}}{\theta} \quad (2)$$

where M_b is the overturning moment at the base of the wall, $M_{BRB,tens}$ and $M_{BRB,comp}$ are respectively the moment contributions due to the BRB in tension and compression, M_{PT} is the moment contributions due to the PT rods, M_{wood} is the moment contribution due to wood in compression at the wall toe. The moment contributions are calculated considering the forces associated with the yielding of the BRB in tension and relative to the center of rotation, which is taken as the center of the wall (Shen *et al*. 2022). The calculations assume the PT forces act at the wall center and the BRB forces act at the wall edges. The base rotation θ is calculated based on the deformations of the BRB in tension at yielding. The variables in (2) depend on the length of the compression zone at the wall toe (c), which is determined from the equilibrium of the vertical forces at yielding of the BRB in tension. Figure 1 (b) shows a schematic of the considered forces at the rocking interface. Future work will incorporate more detailed discussion of the assumptions used to calculate k_r.

To estimate the modal periods ($T_{n,ba}$), the proposed estimating method combines the contribution of the flexural and shear beam as follows (Goel & Chopra 1998):

$$T_{n,ba} = \sqrt{T_{n,f}^2 + T_{n,v}^2} \quad (3)$$

where $T_{n,f}$ is the period of the pure flexural beam with a rotational spring at the base of stiffness k_r calculated from Eq. (2) (Wiebe *et al.* 2015), and $T_{n,v}$ is the period of the pure shear beam with a fixed base (Chopra 2011).

Mass timber has a relatively low shear-to-Young's modulus ratio (G/E≈1/20) depending on various factors such as the direction of loading, the orthotropic properties of the mass timber panels, and the level of deformation. Consequently, the contribution of shear behavior to the structural period is not negligible. In this

study, the estimates of the modal periods combine both flexural and shear behaviour, while the mode shapes estimates are based on flexural behaviour only. Future work will incorporate the shear contribution to the mode shape estimates.

3.2 Stiffness and strength checks

After estimating the mode shapes and modal periods, stiffness, and strength check of the wall are performed.

The stiffness check aims to ensure that the story drift ratios of the mass timber rocking wall at the DE level are below the target of 2% in ASCE 7 (2022). The roof displacement demand ($u_{R,lim}$) at 2% roof drift ratio is calculated assuming a rigid-body rocking response and then converted to an elastic displacement (D_1) associated with the equivalent elastic single degree of freedom oscillator (ASCE 41 2017). The fundamental period ($T_{1,max}$) associated with D_1 is defined from the displacement spectrum at the DE level. To meet the stiffness check, the estimates of the first-mode period ($T_{1,ba}$) from Eq.(3), must be shorter than the maximum period ($T_{1,max}$).

The strength check aims to ensure that the demands on the wall at MCE_R in terms of shear forces and moments are below the nominal capacity of the wall. The design forces for the rocking walls consist of two contributions: i) the first mode force demands which arise from the inelastic forces of the BRBs and the elastic forces in the PT rods; they are limited by the strength of the BRB which slowly increase after yielding, ii) the higher modes force demands which arise from additional inertial forces provided by the wall that remain elastic; they increase near-linearly with displacement and they are referred as *near-elastic higher-mode effects*. For each mode (n), the peak floor displacements and the equivalent floor forces are calculated based on the spectral displacement and accelerations at the MCE_R level and the modal properties (Chopra 2011). Additionally, story drift ratios (θ), story shears (V), and story overturning moments (M) are computed based on the floor forces.

Herein, the Modal Response Spectrum Analysis (MRSA) is applied with the Modal Superposition method, which assumes that near-elastic higher-mode responses are superimposed onto the first mode inelastic response (Martin & Deierlein 2019). Estimates of peak demands (r_i) such as story shear and story overturning moment, at the MCE_R level, are computed as follows:

$$r_i = \left|\frac{r_{i,1}}{R_1}\right| + \sqrt{\sum_{n=2}^{N} (r_{i,n})^2} \tag{4}$$

where i is the story, $r_{i,1}$ is the elastic response in the first mode based on the MCE_R hazard spectrum, which is divided by a first-mode inelastic reduction factor (R_1) to estimate the inelastic response, $r_{i,1}$ is the elastic response in the higher modes based on the MCE_R hazard spectrum. The first-mode inelastic reduction factor (R_1) is defined as follows (Martin & Deierlein 2019):

$$R_1 = \frac{M_{elastic,1}}{M_{MCE}} \tag{5}$$

where M_{MCE} is the overturning moment resistance calculated through a plastic analysis with the MCE_R roof drift ratio, $M_{elastic,1}$ is the first-mode elastic moment demand at MCE_R. At the MCE_R level, the BRBs are expected to yield while the PT rods remain elastic.

In this study, estimates of peak displacements are computed using Eq.(4) and assuming the equal-displacement rule to calculate inelastic displacements in the first mode. Past studies have demonstrated that the inelastic displacement of self-centering systems may be different from the equivalent elastic displacement depending on the hysteretic properties (*i.e.*, ductility, post-hardening ratio) (Pieroni *et al.,* 2022). Future work will incorporate estimates of the peak displacements considering these aspects.

The proposed application of Modal Superposition is consistent with others (Wiebe *et al.* 2015, Martin & Deierlein 2019, Simpson 2020). When applying MRSA, the algebraic signs of the total response are lost through the modal combination, and the combined response parameters do not satisfy equilibrium.

4 Application to a 6-story mass timber building

The proposed estimating method was applied to the design of a 6-story mass timber archetype that was tested at the Large High Performance Outdoor Shake Table (LHPOST) at the University of California San Diego (UCSD) in January 2024 as part of the NHERI Converging Design Project. The building is assumed to be located at a Class C soil site in the Capitol Hill neighborhood of Seattle, Washington (coordinates: 47.6156, -122.3197). The floor plan is approximately square, measuring 10.51 m by 10.46 m [34 ft' – 6 in by 34 ft – 4 in], and the inter-story height is 3.35 m [11 ft], except for the first floor, which is approximately 3.96 m [13']. The seismic-resisting system of the building combines mass timber diaphragms with Post-Tensioned Mass Timber Rocking Walls in both the East-West (E-W) and North-South (N-S) directions. The E-W walls are constructed using Cross-Laminated Timber (CLT) panels, while the N-S walls are made of Mass Ply Panel (MPP). These walls are connected to the diaphragms using shear-key connections designed to transfer shear forces exclusively, allowing for rotation and vertical displacement of the walls relative to the diaphragms. The plan view of the 6-story mass timber building can be found in Wichman *et al.* 2022b.

The NHERI Converging Design Project tested three different seismic-resisting systems (NHERI Converging Design Website). The present study focuses on the seismic-resisting system used for Phase 2 in the N-S direction that features Post-Tensioned rocking MPP walls with BRBs boundary elements (Figure 3).

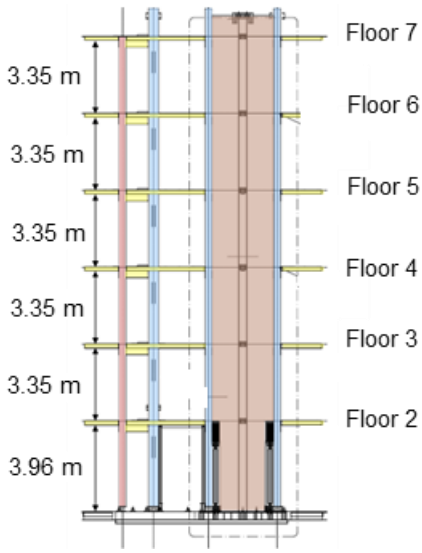

Figure 3. Elevation view of Post-Tensioned Rocking Mass Timber Walls with BRBs boundary elements.

4.1 Sizing of the energy dissipators and PT rods

The width of the MPP wall was chosen based on architectural considerations and to accommodate the BRBs, resulting in a width of d_{w1}=1.96 m [77.25 in] for the first story, and a typical width of d_{wt}=2.64 m [104.25 in] for the higher stories.

The BRB energy dissipators and PT rods were sized considering minimum strength requirements from the design forces using the Equivalent Lateral Force Procedure at DE (ASCE 7 (2022)). An R factor of 8 was assumed for the DE to be consistent with BRB frames. Future work needs to validate this selected R-value. BRBs were selected with a nominal yield strength of 262 MPa [38 ksi] and an expected yield strength of 317 MPa [46 ksi]. Due to constraints related to the available dimensions of BRBs, the yielding area was taken as $A_{r,BRB}$=1,290 mm^2 [2 in^2], which is greater than the required from the calculation ($A_{r,BRB}$ ≥620 mm^2 [0.96 in^2]). The yielding length was calculated as $L_{y,BRB}$=1.93 m [76 in], considering a limit tensile strain demands in the yielding core of 2.5% at the DE level to mitigate low-cycle fatigue (ASCE 41(2017)).

The PT rods were selected with a nominal yield strength of 752 MPa [105 ksi] and an expected yield strength of 896 MPa [125 ksi]. To balance the moment contribution of the BRBs after yielding considering overstrength (Busch *et al.* 2022, Pampanin *et al.* 2001, Palermo 2007), four PT rods with diameter D_{PT}=31.75 mm [1.125 in] were chosen with an initial post-tensioning force T_{PTi}= 981 kN [220 kip]. A smaller pretension force could be assumed if considering the self-weight of the wall and the increase in post-tensioning force due to elongation during rocking.

4.2 Estimates of the mode shapes and modal periods

The estimates of the mode shapes and modal periods associated with the first and second modes are defined according to Eq. (1), considering a constant width of the wall along the height equal to $d_{w,t}$. The elastic modulus of the wall was assumed to be E_w=10945 MPa [1600 ksi] (Soti 2021, Ho 2022). The thickness of the wall was then sized based on the stiffness check to achieve a 2% roof drift ratio at DE, resulting in a thickness of t_w=0.23 m [9.1875 in].

Based on the equilibrium of the vertical forces at the yielding of the BRB in tension, the length of the compression zone in the wood at the wall toe is c=0.41 m [16.12 in], and the associated rotation at the base is θ=0.18% rad. Using (2), the stiffness of the rotation spring at the base of the pure flexural cantilever beam is k_r= 1.16 kNm [10.2 kip in]. Table 1 and Table 2 summarise the estimates for the mode shapes and modal periods.

Table 1. Application of the beam analogy.

Flexural beam with a rotational spring of stiffness (k_r) at the base			Shear beam fixed at the base		
	Mode 1	Mode 2		Mode 1	Mode 2
$\beta_n h$	1.65	4.30	βh	1.57	4.71
T_{nf}	0.95 s	0.14 s	T_{nv}	0.31	0.10

Table 2. Estimate of modal periods and mode shapes using the beam analogy.

	Rocking wall with controlled overturning moments							
n	T_{ba}**	$\phi_{n,1}$*	$\phi_{n,2}$*	$\phi_{n,3}$*	$\phi_{n,4}$*	$\phi_{n,5}$*	$\phi_{n,6}$*	$\phi_{n,7}$*
Mode 1	1.00 s	0.000	0.108	0.248	0.417	0.604	0.801	1.000
Mode 2	0.17 s	0.000	0.408	0.675	0.655	0.300	-0.302	-1.000

** The estimates of the modal period combine both flexural and shear behaviour.

* The estimates of the mode shapes consider flexural behaviour only. Future work will incorporate the shear contribution.

4.3 Stiffness and strength checks

For stiffness checks The modal period associated with the target story drift ratio of 2% at DE is $T_{1,max}$=2.15 s, which is larger than the estimate of the first vibration period $T_{1,ba}$=1.00 s, ensuring that the story drift ratios of the wall at the DE level are below the target of 2% in ASCE 7 (2022).

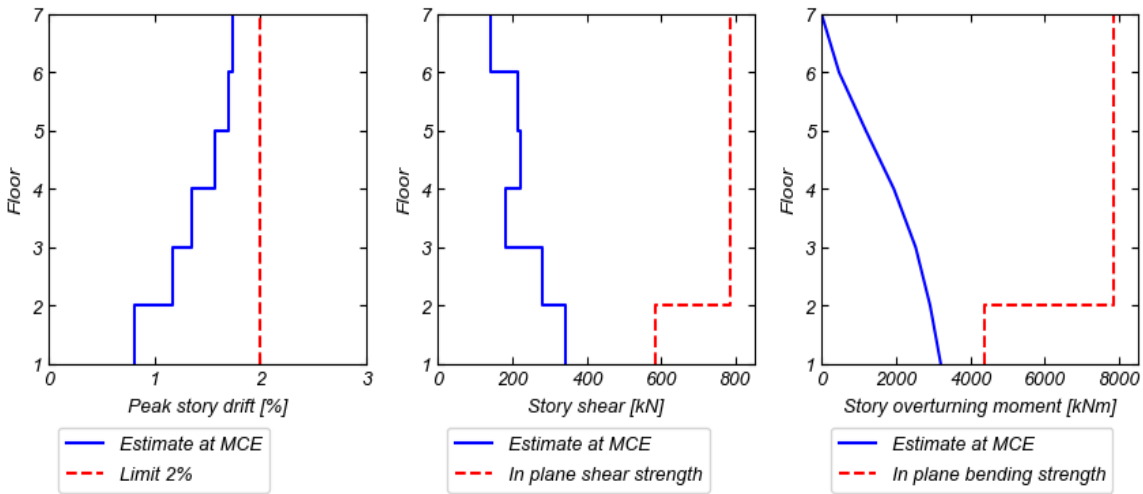

(a) (b) (c)

Figure 4. Estimates of demands using the Modal Response Spectrum Analysis: (a) peak story drifts, (b) story shear, (c) story overturning moment.

For strength checks, results of the MRSA in terms of peak story drifts (θ), shear forces (V), and story overturning moments (M) demands are shown in Figure 4 (a), (b), and (c). The demands are below the flexural

and shear capacity of the wall of M_{wr}= 4369 kNm [38677 kip in] and V_r= 585 kN. [131.52 kip] at the first story, and M_{wr}= 7849 kNm [69474 kip in] and V_r= 784 kN. [176 kip] at the higher story. Additionally, the peak story drift ratios at the MCE_R level are below 2%, which is the limit at the DE level.

5 Verification of the mode shapes and modal periods

To compare the estimate of mode shapes and modal periods, a two-dimensional (2D) finite element model was developed in OpenSeesPy (McKenna *et al.* 2010).

5.1 Numerical model

The MPP walls were modeled using elastic beam-column elements along the height of the building aggregated with the shear material. Nonlinear springs were placed between the base of the wall and the foundation to represent the rocking behaviour and any potential inelasticity due to panel crushing and gap opening at the base of the wall. The nonlinear base springs consisted of zero-length, elastic-perfectly plastic elements along the width and thickness of the wall. The springs work only in compression, assuming the compression strength in the major direction of the wall as the elastic limit and considering a plastic hinge length of two times the thickness. The springs were located based on the Gauss-Legendre quadrature points. The BRBs were modeled as corotational truss elements with a modified stiffness to represent the transition regions from the BRB core. To represent an asymmetric kinematic and isotropic hardening of the BRBs in tension and compression, the uniaxial material model (*Steel04*) was used for the truss elements (Zsarnóczay 2013). Low-cycle fatigue of the BRBs is estimated by accumulating damage using Miner's rule and a Coffin-Manson log-log relationship (Uriz and Mahin 2008). The properties used in the model were calibrated by using test data provided by the industry partner (Araújo *et al.* 2022). The post-tensioned rods were modeled as trusses with an initial strain based on the design post-tensioning force and a tension-only Menegotto-Pinto material (*Steel02)*. The columns of the gravity system were modeled using elastic Timoshenko beam-column elements with equivalent section properties. $P-\Delta$ effects were modeled using a $P-\Delta$ transformation. The leaning columns were constrained horizontally to the wall.

1.1 Eigenvalue analysis and comparison with the estimates

For each mode (n), mode shapes (ϕ_n) and modal periods (T_n) were defined through an eigenvalue analysis using the numerical model, and then compared to the estimates from Eq.(1) and Eq.(3). To align to the estimates, the eigenvalue analysis was performed considering the stiffness of the structure after yielding of the BRB (K_y) in tension rather than the initial stiffness (K_{in}).

Three versions of the 2D model were investigated. Table 3 summarises the properties of the different models: Model 1 (M1) and Model 2 (M2) are simplified versions that simulate the assumptions of the cantilever beam analogy; Model 3 (M3) is the most complete version that best represents the building and features the details described for the numerical model.

Table 3 shows the first modal period based on the initial stiffness ($T_{1,kin}$) and the first and second modal periods based on the stiffness after yielding of the BRB in tension ($T_{1,ky}$, $T_{2,ky}$).

Model 1 (M1) best represents the assumptions made to estimate the mode shapes as it only accounts for the flexural properties of the wall. Figure 5 shows the mode shapes obtained from M1 (green line), M3 (blue line), and the estimates of the mode shape (red line) from Eq.(1). Additionally, the mode shapes of the pure-flexural beam fixed and pinned at the base are shown as references (dotted and dot-dashed black lines). Estimates of the mode shapes align with M1 and are a good approximation of M3.

Model 2 (M2) best represents the assumptions made to estimate the modal periods, as it combines the flexural and shear properties of the wall. It can be observed that the modal estimates (*i.e.*, $T_{1,ba}$=1.00 s, $T_{2,ba}$=0.17 s) are close to the results from the eigenvalue analyses (*i.e.,* $T_{1,ba}$=0.99 s and $T_{2,ba}$=0.15 s).

Note that the behaviour of the rocking wall closely resembles that of a flexural beam fixed at the base at the point when the BRB in tension yields. However, the behaviour depends also on whether the gap-opening mechanics activates or not, resulting in changes to the mode shapes and modal periods. Thus, at larger drift levels, the wall could exhibit behaviour more akin to a pinned connection. Future work will address this aspect more in detail.

Table 3. Properties of the investigated models and results from the eigenvalue analysis.

Properties	M1	M2	M3
G	10^6	73.91	73.91
Wall width	$b_{w1} = b_{w,t}$	$b_{w1} = b_{w,t}$	$b_{w1} \neq b_{w,t}$
Mass*	Distributed	Distributed	Lumped
P-Delta	No	No	Yes
Gravity Frame	No	No	Yes
Material BRBs	Bilinear	Bilinear	Steel 04
$T_{1,kin}$	0.71	0.77	0.97
$T_{1,ky}$ [s]	0.99	1.03	1.34
$T_{2,ky}$ [s]	0.15	0.19	0.22

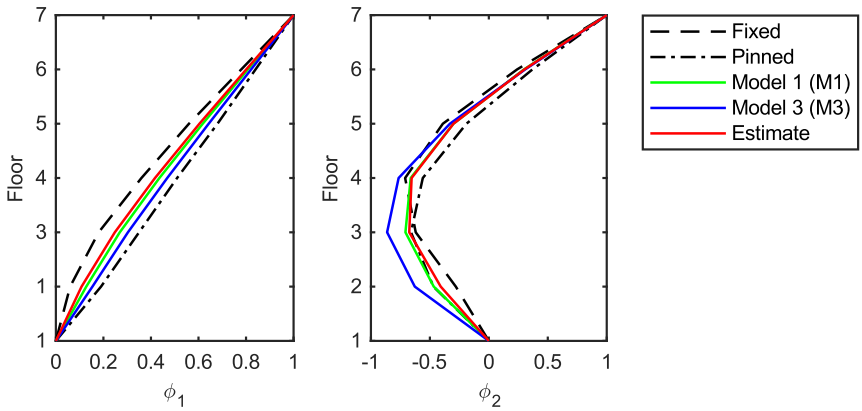

Figure 5. Comparison between the estimates and the mode shapes from the eigenvalue analysis at yielding of the BRB in tension.

2 Summary and Conclusions

First and higher-mode demands were estimated for the design of Post-Tensioned Mass Timber Rocking Walls supplemented with Buckling-Restrained Brace (BRB) boundary elements. To this purpose, estimates of mode shapes and vibration periods were proposed based on a cantilever beam analogy and separating the behaviour of the wall into two components: (i) a pure-flexural cantilever beam restrained at the base by a rotational spring, (ii) a pure-shear cantilever beam fixed at the base. Stiffness and strength checks on the rocking wall were conducted using a Modal Response Spectrum Analysis with a Modal Superposition combination rule, modified to account for the yielding of the BRB in the first mode and the elastic forces in the wall in the higher modes. The proposed estimating method was applied to a 6-story mass timber archetype, tested at the Large High Performance Outdoor Shake Table (LHPOST) at the University of California San Diego (UCSD) in January 2024 as part of the Natural Hazards Engineering Research Infrastructure (NHERI) Converging Design Project. A two-dimensional numerical model was developed in OpenSeesPy to compare the modal periods and mode shapes obtained from the proposed estimating method and from the eigenvalue analysis using models of varying complexity. Results show that the estimates are a good approximation of the behaviour of the wall.

Future developments will incorporate both the flexural and shear behaviour in the estimate of the mode shapes, compare estimates of the demands to nonlinear response history analyses, apply the proposed estimating method to different archetypes, and extend the design procedure to pivoting mass timber walls with controlled overturning moments.

3 Acknowledgments

This material is based upon work supported by the National Science Foundation (NSF) under awards #2120683, #2120692, and #2120684. The authors would also like to acknowledge the United States Department of Agriculture (USDA) Agricultural Research Service, the TallWood Design Institute, and the industry partners for supporting the experimental program of the six-story NSF NHERI Converging Design tests (NHERI Converging Design Website 2024). The authors also acknowledge the support from the University College London's 22-23 Turing Project under the award number TS-2021-10102, which was funded by the UK's global program to study and work abroad. Any opinions, findings, and conclusions are those of the authors and do not necessarily reflect the views of the supporting agencies.

4 References

Akbas, T., Sause, R., Ricles, J. M., Ganey, R., Berman, J. W., Loftus, S., Dolan, J. D.,Pei, S., van de Lindt, J. W., Blomgren, H.-E. (2017). Analytical and Experimental Lateral-Load Response of Self-Centering Posttensioned CLT Walls. Journal of Structural Engineering, 143(6),04017019.

Araújo R., G. A. (2022). Design, Experimental Testing, and Numerical Analysis of a Three-Story Mass Timber Building with a Pivoting Spine and Buckling-Restrained Energy Dissipators. Master's Thesis, submitted to Oregon State University.

ASCE 41. (2017). Seismic Evaluation and Retrofit of Existing Buildings (ASCE/SEI41-17). In. Reston, VA: American Society of Civil Engineers.

ASCE 7. (2016). Minimum Design Loads and Associated Criteria for Buildings and Other Structures (ASCE/SEI 7-16). In. Reston, VA: American Society of Civil Engineers.

ASCE 7. (2022). Minimum Design Loads and Associated Criteria for Buildings and Other Structures (ASCE/SEI 7-22). In. Reston, VA: American Society of Civil Engineers.

AWC. (2021). SDPWS - Special Design Provisions for Wind and Seismic with Commentary. In (Vol. ANSI/AWC SDPWS). Leesburg, VA: American Wood Council.

Bosco, M., Marino, E. M., Rossi, P. P. (2018). A design procedure for pin-supported rocking buckling-restrained braced frames. Earthquake Engineering & Structural Dynamics, 47(14), 2840-2863.

Busch, A., Zimmerman, R. B., Pei, S., McDonnell, E., Line, P., Huang, D. (2022). Prescriptive Seismic Design Procedure for Post-Tensioned Mass Timber Rocking Walls. Journal of Structural Engineering, 148(3), 04021289.

Chen X, Takeuchi T, Matsui R. (2017) Simplified design procedure for controlled spine frames with energy-dissipating members. Journal of Constructional Steel Research, 135:242-252.

Chen X, Takeuchi T, Matsui R. (2018) Seismic Performance and Evaluation of Controlled Spine Frames Applied in High-rise Buildings. Earthquake Spectra, 34(3):1431-1458.

Chen, Z., Popovski, M., Iqbal, A. (2020). Structural Performance of Post-Tensioned CLT Shear Walls with Energy Dissipators. Journal of Structural Engineering, 146(4), 04020035.

Chopra, A. K. (2011). Dynamics of Structures: Theory and Applications to Earthquake Engineering (4 ed.). Pearson.

Christopoulos C., Zhong C. (2022). Towards understanding, estimating and mitigating higher-mode effects for more resilient tall buildings. Resilient City and Structures, 1(1):54:64.

Cook, D. T., Liel, A. B., Haselton, C. B., Koliou, M. (2022). A framework for operationalizing the assessment of post-earthquake functional recovery of buildings. Earthquake Spectra, 38(3), 1972-2007.

Earthquake Engineering Research Institute. (2019). Functional Recovery: A Conceptual Framework with Policy Options.

Eberhard M.O., Sozen M.A. (1993). Behaviour-based method to determine design shear in earthquake-resistant walls. Journal of Structural Engineering, 119(2):619-640.

Eibl, J., Keintzel E. (1988). Seismic shear forces in RC cantilever shear walls. In Vol. 6 of Proc., 9th World Conf. in Earthquake Engineering, 5–10. Tokyo: International Association for Earthquake Engineering.

FEMA P-2082-1. (2020). NEHRP Recommended Seismic Provisions for New Buildings and Other Structures. Federal Emergency Management Agency.

Goel, R. K., Chopra, A. K. (1998). Period Formulas for Concrete Shear Wall Buildings. Journal of Structural Engineering, 124(4), 426-433.

Granello, G., Palermo, A., Pampanin, S., Pei, S., Van de Lindt, J. (2020). Pres-Lam Buildings: State-of-the-Art. Journal of Structural Engineering, 146(6). 04020085

Ho, X. T., A. Arora, and A. Sinha. (2022). In-plane shear properties of mass ply panels in long-ply direction. Journal of Materials in Civil Engineering, 34(8).

Huang, D., Pei, S., Busch, A. (2021). Optimizing displacement-based seismic design of mass timber rocking walls using genetic algorithm. Engineering Structures, 229, 111603.

IBC. (2020). 2021 International Building Code. In. USA: International Code Council, Inc.

Jiang, Q., Wang, H., Feng, Y., Chong, X., Huang, J., Wang, S., Zhou, Y. (2022). Analysis and experimental testing of a self-centering controlled rocking wall with buckling-restrained braces at base. Engineering Structures, 269, 114843.

Loo, W. Y., Kun, C., Quenneville, P., Chouw, N. (2014). Experimental testing of a rocking timber shear wall with slip-friction connectors. Earthquake Engineering & Structural Dynamics, 43(11), 1621-1639.

Loss, C., Tannert, T., Tesfamariam, S. (2018). State-of-the-art review of displacement-based seismic design of timber buildings. Construction and Building Materials, 191, 481-497.

Martin, A., Deierlein, G. G., Ma, X. (2019). Capacity Design Procedure for Rocking Braced Frames Using Modified Modal Superposition Method. Journal of Structural Engineering, 145(6), 04019041.

McKenna, F., Scott, M. H., Fenves, G. L. (2010). Nonlinear Finite-Element Analysis Software Architecture Using Object Composition. Journal of Computing in Civil Engineering, 24(1), 95-107.

Molina Hutt, C., Hulsey, A. M., Kakoty, P., Deierlein, G. G., Eksir Monfared, A., Wen-Yi, Y., Hooper, J. D. (2022). Toward functional recovery performance in the seismic design of modern tall buildings. Earthquake Spectra, 38(1), 283-309.

NHERI Converging Design Website (2023). URL: https://tallwoodinstitute.org/converging-design-home-5663/, accessed January 22, 2024.

Palermo, A., Pampanin, S., Marriott, D. (2007). Design, Modeling, and Experimental Response of Seismic Resistant Bridge Piers with Posttensioned Dissipating Connections. Journal of Structural Engineering, 133(11), 1648-1661.

Pampanin S., Priestley M.J.N., Sritharan S. (2001). Analytical modelling of the seismic behaviour of precast concrete frames designed with ductile connections. Journal of Earthquake Engineering, 2001, 329-367

Panagiotou M, Restrepo J. I. (2009). Dual-plastic hinge design concept for reducing higher-mode effects on high-rise cantilever wall buildings. Earthquake Engineering & Structural Dynamics, 38(12):1359–80.

Panagiotou M, Restrepo J. I. (2011). Displacement-based method of analysis for regular reinforced-concrete wall buildings: application to a full-scale 7-story building slice tested at UC–San Diego. Journal of Structural Engineering, 137(6):677-690.

Panagiotou, M., Restrepo, J. I., Conte, J. P. (2011). Shake-Table Test of a Full-Scale 7-Story Building Slice. Phase I: Rectangular Wall. Journal of Structural Engineering, 137(6), 691-704.

Pang, W., Rosowsky, D. V., Pei, S., van de Lindt, J. W. (2010). Simplified direct displacement design of six-story woodframe building and pretest seismic performance assessment. Journal of Structural Engineering, 136(7), 813-825.

Pei, S., van de Lindt, J. W., Barbosa, A. R., Berman, J. W., McDonnell, E., Dolan, J.D., Blomgren, H.-E., Zimmerman, R. B., Huang, D., Wichman, S. (2019). Experimental Seismic Response of a Resilient 2-Story Mass-Timber Building with Post-Tensioned Rocking Walls. Journal of Structural Engineering, 145(11), 04019120.

Pieroni, L., Freddi, F., Latour, M. (2022). Effective placement of self-centering damage-free connections for seismic-resilient steel moment resisting frames, Earthquake Engineering & Structural Dynamics. 51 (2022) 1292–1316.

Restrepo J. I., Rahman A. (2007). Seismic Performance of Self-Centering Structural Walls Incorporating Energy Dissipators. Journal of Structural Engineering, 133(11), 1560-1570.

Roke D., Sause R., Ricles J.M., Gonner N. (2009). Design Concepts for Damage-Free Seismic-Resistant Self-Centering Steel Concentrically Braced Frames. Structures Congress 2009: Don't Mess with Structural Engineers: Expanding Our Role.

Sanscartier Pilon, D., Palermo, A., Sarti, F., Salenikovich, A. (2019). Benefits of multiple rocking segments for CLT and LVL Pres-Lam wall systems. Soil Dynamics and Earthquake Engineering, 117, 234-244

Sarti, F., Palermo, A., Pampanin, S. (2016). Quasi-Static Cyclic Testing of Two-Thirds Scale Unbonded Posttensioned Rocking Dissipative Timber Walls. Journal of Structural Engineering, 142(4), E4015005.

Shen, Y., Fredddi, F., Li, Y., Li, J. (2022). Parametric experimental investigation of unbonded post-tensioned reinforced concrete bridge piers under cyclic loading, Earthquake Engineering & Structural Dynamics, 51(15), 3457-3778

Simpson, B.G. (2020). Higher-mode force response in multi-story strongback-braced frames. Earthquake Engineering & Structural Dynamics, 49(14), 1406-1427.

Simpson, B. G., Mahin, S. A. (2018). Experimental and Numerical Investigation of Strongback Braced Frame System to Mitigate Weak Story Behaviour. Journal of Structural Engineering, 144(2), 04017211.

Simpson, B. G., Rivera Torres, D. (2021). Simplified Modal Pushover Analysis to Estimate First- and Higher-Mode Force Demands for Design of Strongback-Braced Frames. Journal of Structural Engineering, 147(12), 04021196.

Soti, R., T. X. Ho, and A. Sinha. (2021). Structural performance characterization of mass plywood panels. Journal of Materials in Civil Engineering, 33(10):04021275.

Steele, T. C., Wiebe, L. D. A. (2016). Dynamic and equivalent static procedures for capacity design of controlled rocking steel braced frames. Earthquake Engineering & Structural Dynamics, 45(14), 2349-2369.

Takeuchi, T., Chen, X., Matsui, R. (2015). Seismic performance of controlled spine frames with energy-dissipating members. Journal of Constructional Steel Research, 114, 51-65.

Terzic, V., Villanueva, P.K., Saldana D., Yoo D.Y. (2021). F-Rec Framework: Novel Framework for Probabilistic Evaluation of Functional Recovery of Building Systems. PEER Report No. 2021/06.

Tremblay, R., Chen, L., Tirca, L. (2014). Enhancing the Seismic Performance of Multi-storey Buildings with a Modular Tied Braced Frame System with Added Energy Dissipating Devices. International Journal of High-Rise Buildings, 3(1), 21-33.

Uarac, P., Barbosa, A.R., Brown, N. C., Ho, T., Kontra, S., Simpson, B., Sinha, A., Van de Lindt, J.W. (2022) Direct Displacement Design of Post-Tensioned Mass Timber Rocking Walls with Dissipative Systems. International Mass Timber Conference, Portland, OR. (poster).

Uriz, P., Mahin, S. A. (2008). Toward Earthquake-Resistant Design of Concentrically Braced Steel-Frame Structures (PEER Report 2008/08, Issue).

Wichman, S., Berman, J. W. Pei, S. (2022a). Experimental investigation and numerical modeling of rocking cross laminated timber walls on a flexible foundation. Earthquake Engineering & Structural Dynamics, 51(7), 1697-1717.

Wichman, S., Berman, J. W., Zimmerman, R. B., Pei, S. (2022b). Lateral Design of a 10-Story Building Specimen with Mass Timber Rocking Walls 12th National Conference on Earthquake Engineering, Salt Lake City, UT.

Wiebe, L., Christopoulos, C. (2009). Mitigation of Higher Mode Effects in Base-Rocking Systems by Using Multiple Rocking Sections. Journal of Earthquake Engineering, 13, 83-108.

Wiebe, L., Christopoulos, C. (2015). A cantilever beam analogy for quantifying higher mode effects in multistorey buildings. Earthquake Engineering & Structural Dynamics, 44(11), 1697-1716.

Yassin, A., Ezzeldin, M., Wiebe, L. (2022). Experimental Assessment of Controlled Rocking Masonry Shear Walls without Post-tensioning. Journal of Structural Engineering, 148(4), 04022018.

Zsarnóczay, Á. (2013). Experimental and Numerical Investigation of Buckling Restrained Braced Frames for Eurocode Conform Design Procedure Development. PhD dissertation submitted to Budapest University of Technology and Economics.